Stiffness of Planar 2-DOF 3-Differential Cable-Driven Parallel Robots

Lionel Birglen, Marc Gouttefarde

Stiffness of Planar 2-DOF 3-Differential Cable-Driven Parallel Robots

Lionel Birglen[1] and Marc Gouttefarde[2]

[1]Department of Mechanical Engineering, Polytechnique Montréal, QC, Canada
[2]LIRMM, University of Montpellier, CNRS, Montpellier, France
lionel.birglen@polymtl.ca, marc.gouttefarde@lirmm.fr

Abstract. Planar 2-degree-of-freedom (DOF) 3-differential Cable-Driven Parallel Robots (CDPRs) consist of a point-mass end-effector driven by a number of cables. Each cable is divided into four segments, three of them being connected to the point-mass end-effector by means of routing pulleys. This paper deals with the stiffness analysis of such planar 2-DOF 3-differential CDPRs. Based on the usual linear spring cable elongation model, the expression of the stiffness matrix is derived. The stiffness and workspace of several examples of planar 2-DOF 3-differential CDPRs are then compared. The results of these comparisons illustrate that the stiffness of planar CDPRs can be significantly improved by means of pulley differentials.

Keywords: Cable-driven parallel robots, differential pulley actuation, stiffness analysis

1 Introduction

This paper deals with cable-driven parallel robots (CDPRs) whose cable segments are not each driven by a single actuator but are coupled through differentials. Coupling and transmitting the actuation torque of a single actuator to several cable segments has been shown in previous works to be a possible solution to extend the workspace of CDPRs by purely passive mechanical means [1–3], i.e. without relying on additional actuators or relocating the latter on a structural frame. Compared to conventional CDPRs, more cable segments then cluttered the workspace but this should not be a critical issue for planar and suspended CDPRs. In the specific example studied here, a single actuator simultaneously controls the lengths of three cable segments going from the ground to the point-mass end-effector of a planar robot and the coupling between these cable segments is implemented through pulley differentials, similarly in principle to the well-known block and tackle. The present paper presents and quantifies the stiffness of such planar 2-DOF 3-differential CDPRs. Such differential couplings will be shown to provide a noticeable improvement in the stiffness of the CDPR.

As shown in Fig. 1, each cable of the CDPR consists of four successive segments B_iP, PE_i, E_iM_i, and M_iP. Three of these cable segments link the point

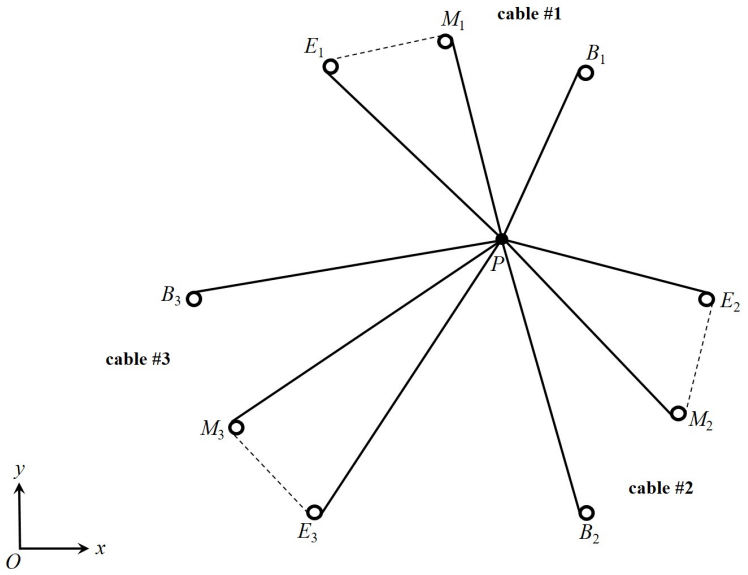

Fig. 1. A planar 2-DOF 3-Differential CDPR where each cable consists of four segments B_iP_i, P_iE_i, E_iM_i, and M_iP_i, three of these segments connecting the end-effector P to the ground points B_i, M_i and E_i.

mass P, which plays the role of the CDPR 2-DOF end-effector, to the ground. In the remainder of this paper, these three segments are referred to as the *active cable segments*. The other one, E_iM_i, extends between points E_i and M_i which are both fixed to the ground. In other words, cable i exits the base first at point B_i, and then goes in this order through points P, E_i, M_i to finally be attached to point P. Hence, these pulley drives are referred to as 3-differential since each one has three "active" outputs. Figure 2 shows this cable routing. In order to implement such a mechanism, pulleys need to be used at points P, E_i, and M_i. However, as a first approximation, the diameters of these pulleys are neglected (considered to be null) and pulley friction is ignored (no friction). The latter assumption implies that the cable tension is constant all along the cable, i.e., the four cable segments have the same tension and each active segment applies a force of identical magnitude on the end-effector. Let n be the number of cables used to drive point P ($n = 3$ in the case of Fig. 1). This paper deals with the case of planar 2-DOF 3-differential CDPRs with $n \geq 2$ cables. The mass of the cables is neglected and all the cable segments are considered to be straight line segments.

Stiffness and vibration analyses of usual CDPRs, where the driving cables are directly attached to the end-effector, have been proposed in a number of works, e.g. [4–11]. As previously mentioned, the main difference with these previous works is that the present paper deals with the stiffness analysis of planar point-

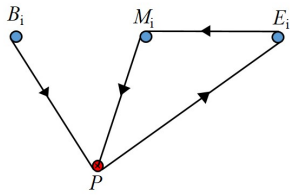

Fig. 2. Cable routing in a single differential: The cable starts at point B_i where the actuated drum is located, goes to P (the end-effector), then to E_i where it is redirected to point M_i in order to be finally attached to point P.

mass CDPRs with 3-differential pulley drive. To the best of our knowledge, the only previous work on stiffness analysis of differential-pulley planar CDPRs is [12] where the case of cables with two active segments is considered. Moreover, the stiffness analysis in [12] only considered stiffness in a single direction and did not mention the trade-off between the size of the workspace and the improvement in stiffness inherent to pulley differentials as will be shown here.

This paper is organized as follows: First, Section 2 presents the Jacobian and wrench matrices of differential-pulley-driven planar point-mass CDPRs with three active cable segments. Then, in Section 3, the stiffness matrix of these mechanisms is derived based on the usual linear spring cable elongation model. Finally, Section 4 reports simulations of the resulting stiffness of several examples of planar 2-DOF 3-differential CDPRs.

2 Wrench and Jacobian Matrices

The active length of the cable i in each differential routing is defined as $l_i = l_{B_iP}+l_{E_iP}+l_{M_iP}$ where $l_{B_iP} = \|\overrightarrow{B_iP}\|$, $l_{E_iP} = \|\overrightarrow{E_iP}\|$ and $l_{M_iP} = \|\overrightarrow{M_iP}\|$ are the strained lengths of the active cable segments B_iP, E_iP and M_iP, respectively. Length l_i is the sum of the cable segment lengths that change when the position of point P changes. It should not be confused with the total length of the cable which includes the length of the cable segment between points E_i and M_i. Let us define the vector $\mathbf{l}$ of the active cable lengths l_i as $\mathbf{l} = [l_1, l_2, \ldots, l_n]^T$. Moreover, let $\dot{\mathbf{l}}$ be the time derivative of $\mathbf{l}$, $\mathbf{p} = [p_x, p_y]^T$ be the position vector of point P in the fixed reference frame $(0, x, y)$, and $\dot{\mathbf{p}}$ the velocity of point P. A Jacobian matrix $\mathbf{J}$ then maps $\dot{\mathbf{p}}$ (resp. $d\mathbf{p}$) into $\dot{\mathbf{l}}$ (resp. $d\mathbf{l}$)

$$\dot{\mathbf{l}} = \begin{bmatrix} \dot{l}_1 \\ \dot{l}_2 \\ \vdots \\ \dot{l}_n \end{bmatrix} = \mathbf{J}\dot{\mathbf{p}} \quad \Longleftrightarrow \quad d\mathbf{l} = \mathbf{J}d\mathbf{p} \tag{1}$$

with

$$\mathbf{J} = \begin{bmatrix} \mathbf{u}_{B1}^T + \mathbf{u}_{E1}^T + \mathbf{u}_{M1}^T \\ \vdots \\ \mathbf{u}_{Bn}^T + \mathbf{u}_{En}^T + \mathbf{u}_{Mn}^T \end{bmatrix}_{n\times 2} \tag{2}$$

where $\mathbf{u}_{Bi}$, $\mathbf{u}_{Ei}$ and $\mathbf{u}_{Mi}$ are the unit vectors directed along the cable segments B_iP, E_iP, and M_iP, pointing from the base points B_i, E_i, and M_i, to point P, respectively. The vector of cable tensions t_i is denoted $\mathbf{t} = [t_1, t_2, \ldots, t_n]^T$. Pulley friction being neglected, the cable tension t_i is constant all along the cable. The force $\mathbf{f}$ applied by the n cables to the point-mass P is then given by

$$\mathbf{f} = \mathbf{W}\mathbf{t} \tag{3}$$

where the $2 \times n$ wrench matrix $\mathbf{W}$ is defined as $\mathbf{W} = -\mathbf{J}^T$.

3 Stiffness Analysis

The elastic potential energy of cable i is given by

$$V_i = \frac{1}{2} k_i \left(l_{ti} - l_{0i}\right)^2 \tag{4}$$

where l_{ti} is the total length of cable i

$$l_{ti} = l_i + l_{E_iM_i} \tag{5}$$

with $l_{E_iM_i}$ the length of the passive cable segment E_iM_i and $l_i = l_{B_iP} + l_{E_iP} + l_{M_iP}$ the active length of cable i, as defined in Section 2. l_{0i} is the corresponding unstrained length, $l_{0i} = l_{0_{B_iP}} + l_{0_{E_iP}} + l_{0_{E_iM_i}} + l_{0_{M_iP}}$. The elongation is supposed to be uniform along the cable length and the cable is assumed to be a linear spring with $t_i = k_i \left(l_{ti} - l_{0i}\right)$, $k_i = \frac{AE}{l_{0i}}$, where A and E are the cable cross-sectional area and elastic modulus, respectively.

The total elastic potential energy V of the 3-differential CDPR is then the sum of the elastic potential energies of all its n cables

$$V = \sum_{i=1}^{n} V_i = \frac{1}{2} \sum_{i=1}^{n} k_i \left(l_{ti} - l_{0i}\right)^2 \tag{6}$$

Computing the derivative of Equation (6) yields

$$dV = \sum_{i=1}^{n} dV_i = \sum_{i=1}^{n} k_i \left(l_{ti} - l_{0i}\right) dl_{ti} = \sum_{i=1}^{n} k_i \left(l_{ti} - l_{0i}\right) dl_i \tag{7}$$

where $dl_{ti} = dl_i$ according to Eq. (5) and to the fact that $dl_{E_iM_i} = 0$ (the distance between the ground points E_i and M_i is constant). Then, defining the diagonal matrix $\mathbf{D}$ and vectors $\mathbf{l}_t$ and $\mathbf{l}_0$ as follows

$$\mathbf{D} = \begin{bmatrix} k_1 & & \\ & \ddots & \\ & & k_n \end{bmatrix} \quad , \quad \mathbf{l}_t = \begin{bmatrix} l_{t1} \\ l_{t2} \\ \vdots \\ l_{tn} \end{bmatrix} \quad \text{and} \quad \mathbf{l}_0 = \begin{bmatrix} l_{01} \\ l_{02} \\ \vdots \\ l_{0n} \end{bmatrix} \tag{8}$$

Eq. (7) can be written

$$dV = (\mathbf{l}_t - \mathbf{l}_0)^T \mathbf{D} d\mathbf{l} \tag{9}$$

According to Eq. (1), $d\mathbf{l}$ is equal to $\mathbf{J}d\mathbf{p}$ so that according to Eq. (9)

$$\frac{dV}{d\mathbf{p}} = \begin{bmatrix} \dfrac{\partial V}{\partial p_x} \\ \dfrac{\partial V}{\partial p_y} \end{bmatrix} = \mathbf{J}^T \mathbf{D} (\mathbf{l}_t - \mathbf{l}_0) \tag{10}$$

where it can be noted that $\mathbf{D}(\mathbf{l}_t - \mathbf{l}_0) = \mathbf{t}$ since $t_i = k_i (l_{ti} - l_{0i})$. The stiffness matrix $\mathbf{K}$ of the 3-differential CDPR is defined as the second derivative of the elastic potential energy, namely

$$\mathbf{K} = \frac{d^2V}{d\mathbf{p}^2} = \begin{bmatrix} \dfrac{\partial^2 V}{\partial p_x^2} & \dfrac{\partial^2 V}{\partial p_x \partial p_y} \\ \dfrac{\partial^2 V}{\partial p_y \partial p_x} & \dfrac{\partial^2 V}{\partial p_y^2} \end{bmatrix} \tag{11}$$

Taking the derivative of Eq. (10) with respect to $\mathbf{p}$, the following classic expression of the stiffness matrix is obtained

$$\mathbf{K} = \mathbf{J}^T \mathbf{D} \frac{d\mathbf{l}}{d\mathbf{p}} + \frac{d\mathbf{J}^T}{d\mathbf{p}} \mathbf{D} (\mathbf{l}_t - \mathbf{l}_0) = \mathbf{J}^T \mathbf{D} \mathbf{J} + \frac{d\mathbf{J}^T}{d\mathbf{p}} \mathbf{t} \tag{12}$$

where, once again, the equality $d\mathbf{l}_t = d\mathbf{l}$ has been used. It is worth noting that this stiffness matrix $\mathbf{K}$ can only be used in local stiffness analyses because Eq. (12) is obtained from Eq. (10) by assuming that $\mathbf{l}_0$ is constant. In other words, the matrix $\mathbf{K}$ is defined at an equilibrium, defined by both the position $\mathbf{p}$ and the cable tensions $\mathbf{t}$, and it can be used to analyze the stiffness of the robot in the vicinity of this equilibrium. In this local analysis, the actuators are assumed to be locked or their position controlled to a constant value. Note also that, according to Eq. (3) and (10), $\dfrac{dV}{d\mathbf{p}} = \mathbf{J}^T \mathbf{t} = -\mathbf{f}$, and thus

$$\mathbf{K} = \frac{d}{d\mathbf{p}} \left(\frac{dV}{d\mathbf{p}} \right) = \frac{d(-\mathbf{f})}{d\mathbf{p}} \Longleftrightarrow \mathbf{K} d\mathbf{p} = d(-\mathbf{f}) \tag{13}$$

Hence, in the vicinity of an equilibrium defined by $\mathbf{p}$ and $\mathbf{t}$, $\mathbf{K}$ maps an infinitesimal displacement $d\mathbf{p}$ in the position of point P to the corresponding infinitesimal change in the force $-\mathbf{f}$, where $\mathbf{f}$ is the force applied by the cables to point P (Eq. (3)).

The approach used above to derive the stiffness matrix is a rather classic one, but care must be taken to use in Eq. (12) the Jacobian matrix defined in Eq. (1), where each row of this matrix is equal to the sum $\mathbf{u}_{Bi}^T + \mathbf{u}_{Ei}^T + \mathbf{u}_{Mi}^T$ of the unit vectors directed along the three straight line segments delineated by the active cable segments.

Referring to the right-hand side of Eq. (12), the stiffness matrix is seen to be the sum of two matrices. In the next section of this paper, for simplicity and due to space limitations, only the influence on stiffness of the matrix $\mathbf{J}^T\mathbf{D}\mathbf{J}$ will be considered.

4 Results

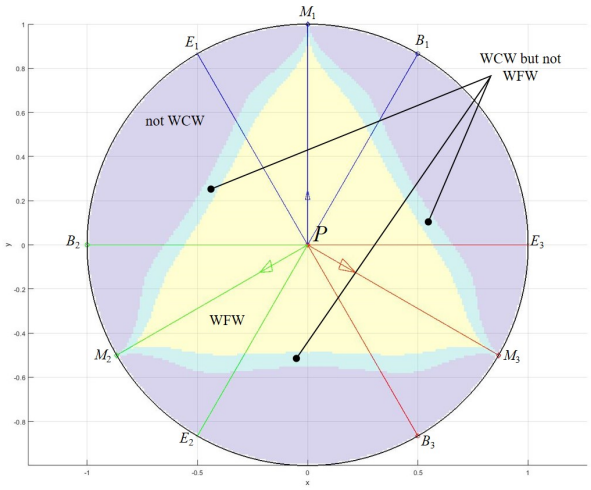

Fig. 3. Example planar 2-DOF 3-differential CDPR with 3 cables (Case 1)

This section reports simulations of the stiffness of six planar 2-DOF 3-differential CDPRs with $n = 3$ cables, across their respective workspaces. These six examples are defined as Cases 1 to 6 in Tables 1 and 2. Case 1 is shown in Fig. 3 together with its Wrench-Closure Workspace (WCW) [13] and Wrench-Feasible Workspace (WFW) [14]. Here, the WFW is defined as the set of positions of point P such that any force $\mathbf{f}$ of magnitude less or equal to 0.1 N can be generated by the cables at P with tensions t_i, $i = 1 \dots n$, satisfying $t_{min} \leq t_i \leq t_{max}$ where $t_{min} = 0.1$ N and $t_{max} = 1$ N.

Case 2 defined in Table 1 is a planar 2-DOF 3-differential CDPR where the three active cable segments are superposed. It is obtained from Case 1 by taking $B_i \equiv E_i \equiv M_i$ for $i = 1, 2$ and 3. Case 3 in Table 1 defines a CDPR without pulley differential where each cable consists of only one segment from B_i to P. It is obtained from Case 1 by keeping segment B_iP and removing the other cable segments PE_i, E_iM_i, and M_iP.

Case 4 defined in Table 2 is another planar 2-DOF 3-differential CDPR. It is shown in Fig. 4 where its WFW is defined as above for Case 1. Case 5 is a planar 2-DOF 3-differential CDPR obtained from Case 4 by superposing the 3

	Case 1		Case 2		Case 3	
	x (m)	y (m)	x (m)	y (m)	x (m)	y (m)
B_1	$\cos(\pi/3)$	$\sin(\pi/3)$	$\cos(\pi/3)$	$\sin(\pi/3)$	$\cos(\pi/3)$	$\sin(\pi/3)$
E_1	$\cos(2\pi/3)$	$\sin(2\pi/3)$	$\cos(\pi/3)$	$\sin(\pi/3)$	$\times$	$\times$
M_1	0	1	$\cos(\pi/3)$	$\sin(\pi/3)$	$\times$	$\times$
B_2	-1	0	-1	0	-1	0
E_2	$\cos(-2\pi/3)$	$\sin(-2\pi/3)$	-1	0	$\times$	$\times$
M_2	$\cos(-5\pi/6)$	$\sin(-5\pi/6)$	-1	0	$\times$	$\times$
B_3	$\cos(-\pi/3)$	$\sin(-\pi/3)$	$\cos(-\pi/3)$	$\sin(-\pi/3)$	$\cos(-\pi/3)$	$\sin(-\pi/3)$
E_3	1	0	$\cos(-\pi/3)$	$\sin(-\pi/3)$	$\times$	$\times$
M_3	$\cos(-\pi/6)$	$\sin(-\pi/6)$	$\cos(-\pi/3)$	$\sin(-\pi/3)$	$\times$	$\times$

Table 1. Geometries of the first three examples of planar 2-DOF 3-differential CDPRs. The crosses $\times$ indicate that the corresponding point E_i or M_i does not exist, i.e., Case 3 defines a CDPR without pulley differential where each cable consists of only one segment from B_i to P.

	Case 4		Case 5		Case 6	
	x (m)	y (m)	x (m)	y (m)	x (m)	y (m)
B_1	1	0	1	0	1	0
E_1	$\cos(2\pi/3)$	$\sin(2\pi/3)$	1	0	$\times$	$\times$
M_1	$\cos(\pi/3)$	$\sin(\pi/3)$	1	0	$\times$	$\times$
B_2	$\cos(2\pi/3)$	$\sin(2\pi/3)$	$\cos(2\pi/3)$	$\sin(2\pi/3)$	$\cos(2\pi/3)$	$\sin(2\pi/3)$
E_2	$\cos(-2\pi/3)$	$\sin(-2\pi/3)$	$\cos(2\pi/3)$	$\sin(2\pi/3)$	$\times$	$\times$
M_2	-1	0	$\cos(2\pi/3)$	$\sin(2\pi/3)$	$\times$	$\times$
B_3	$\cos(-2\pi/3)$	$\sin(-2\pi/3)$	$\cos(-2\pi/3)$	$\sin(-2\pi/3)$	$\cos(-2\pi/3)$	$\sin(-2\pi/3)$
E_3	1	0	$\cos(-2\pi/3)$	$\sin(-2\pi/3)$	$\times$	$\times$
M_3	$\cos(-\pi/3)$	$\sin(-\pi/3)$	$\cos(-2\pi/3)$	$\sin(-2\pi/3)$	$\times$	$\times$

Table 2. Geometries of the last three examples of planar 2-DOF 3-differential CDPRs. Case 6 defines a CDPR without pulley differential where each cable consists of only one segment from B_i to P.

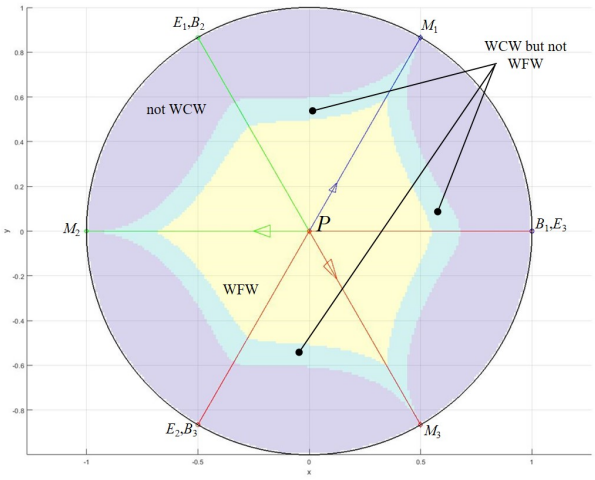

Fig. 4. Example planar 2-DOF 3-differential CDPR with 3 cables (Case 4)

active segments of each cable and Case 6 is a CDPR without pulley differential obtained from Case 4 by removing, for each cable, all segments but B_iP.

As mentioned at the end of Section 3, the subsequent stiffness analysis is based on considering that the stiffness matrix is $\mathbf{K} = \mathbf{J}^T\mathbf{D}\mathbf{J}$. To "normalize" the stiffness coefficient with respect to specific values, we use $E = 1$ Pa and $A = 0.001$ m^2. Note that these values, together with the t_{min} and t_{max} values defined above, do not correspond to actual physical values since, for instance, steel wire ropes typically have elastic modulus E of tens of GPa. However, it is not important for the purposes of this section where stiffness comparisons between several 2-DOF 3-differential CDPRs are made. Moreover, in the calculation of $\mathbf{D}$, for simplicity, we assume that the unstrained length of each cable segment is equal to its strained length. For a given position of the end-effector P, the two eigenvalues of the 2×2 stiffness matrix $\mathbf{K}$ can then be calculated. The minimum (resp. maximum) stiffness values shown in the left part (resp. right part) of Fig. 5 are defined as the minimum (resp. maximum) of these two eigenvalues. The values of the ratios of the minimum to the maximum eigenvalues over the WCW of Case 1 are shown in Fig. 6.

The means of the minimum stiffness values, maximum stiffness values and ratio of minimum to maximum stiffness values over the WCW of the planar 2-DOF 3-differential CDPR examples defined in Tables 1 and 2 are given in Table 3. The mean of the minimal stiffness in Case 1 is 2.4 times larger than in Case 3, where Case 3 corresponds to a classic CDPR with no pulley differential. The means of the maximum stiffness and stiffness ratio in Case 1 are both 1.4 times larger than in Case 3. Comparing Case 2 to Case 3, the minimum and maximum stiffness values are 3 times larger for Case 2 while the stiffness ratios are identical. Hence, planar 2-DOF 3-differential CDPRs (Cases 1 and 2) present a larger stiffness over their workspace than the corresponding CDPR without

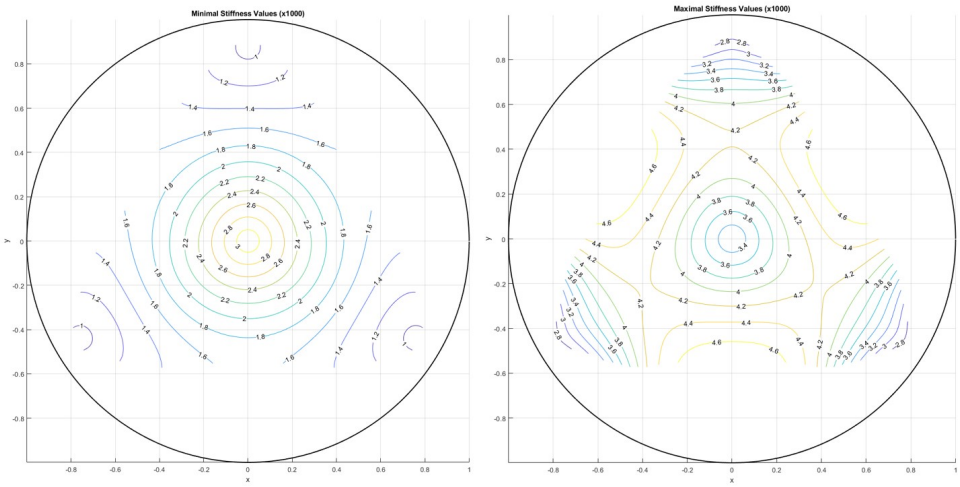

Fig. 5. Minimum and maximum stiffness values over the WCW of Case 1

Case	min (N/m)	max (N/m)	ratio
1	0.0018	0.0041	0.43
2	0.0022	0.0086	0.31
3	0.00074	0.0029	0.31
4	0.0012	0.0016	0.79
5	0.0022	0.0086	0.31
6	0.00074	0.0029	0.31

Table 3. Means of the minimum stiffness values (min), maximum stiffness values (max) and ratio of minimum to maximum stiffness values (ratio) over the WCW of the 2-DOF 3-differential CDPR examples

pulley differential (Case 3). Similar results are obtained by comparing Cases 4 and 5 to Case 6. The cases with superposed cable segments (Cases 2 and 5) have larger minimum and maximum stiffness values than the ones with distinct cable segments (Cases 1 and 4). Note that Case 4 has the best stiffness ratio.

Finally, Table 4 shows a comparison of the size of the WCW and WFW in each case. The WFW is defined for all the six cases as it has been defined above for Case 1. From these examples, it can be concluded that the cases of 2-DOF 3-differential CDPRs with superposed cable segments (Cases 2 and 5) lead to the largest stiffness improvements but with a marginal gain on the sizes of the WCW and WFW, as compared to the cases without pulley differentials (Cases 3 and 6). In comparison, the stiffness improvement is less significant in the cases of 2-DOF 3-differential CDPRs with distinct cable segments (Cases 1 and 4) with, however, a slightly better improvement in the WCW and WFW sizes.

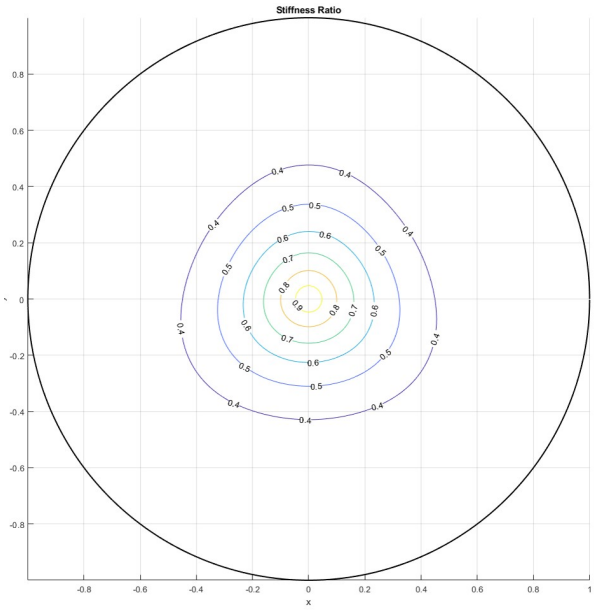

Fig. 6. Ratio of minimal to the maximal stiffness values over the WCW of Case 1

5 Conclusion

This paper presented the stiffness analysis of planar 2-DOF CDPRs with pulley differentials where a single actuator simultaneously controls the lengths of three cable segments going from the ground to the point-mass end-effector. Based on the usual linear spring cable elongation model, the expression of the stiffness matrix has been derived. The stiffness and workspace of several examples of planar 2-DOF 3-differential CDPRs have then been compared. These comparisons show that the stiffness of such planar CDPRs can be significantly improved compared to more common CDPRs without pulley differentials, without decreasing the size of the CDPR workspace. Additionally, the presented example comparisons

Case	WCW	WFW
1	37.6%	29.5%
2	32.4%	27.3%
3	32.4%	24.7%
4	33.6%	22.6%
5	32.4%	27.3%
6	32.4%	24.7%

Table 4. WCW and WFW coverage of the total area occupied by the CDPR examples. This total area is the one delimited by the circles shown in Fig. 3 and 4.

also showed that a trade-off may exist between designing a CDPR with pulley differentials to improve stiffness and designing one to increase the workspace size.

References

1. H. Khakpour, L. Birglen, and S. Tahan, "Synthesis of differentially driven planar cable parallel manipulators," *IEEE Transactions on Robotics*, vol. 30, no. 3, pp. 619–630, June 2014.
2. H. Khakpour and L. Birglen, "Workspace augmentation of spatial 3-dof cable parallel robots using differential actuation," in *2014 IEEE/RSJ International Conference on Intelligent Robots and Systems*, Sept 2014, pp. 3880–3885.
3. H. Khakpour, L. Birglen, and S.-A. Tahan, "Analysis and optimization of a new differentially driven cable parallel robot," *Journal of Mechanisms and Robotics*, vol. 7, no. 3, pp. 034 503–034 503–6, Aug 2015. [Online]. Available: http://dx.doi.org/10.1115/1.4028931
4. S. Behzadipour and A. Khajepour, "Stiffness of cable-based parallel manipulators with application to stability analysis," *ASME J. Mech. Des.*, vol. 128, pp. 303–310, jan 2006.
5. X. Diao and O. Ma, "Vibration analysis of cable-driven parallel manipulators," *Multibody System Dynamics*, vol. 21, pp. 347–360, 2009.
6. M. Arsenault, "Workspace and stiffness analysis of a three-degree-of-freedom spatial cable-suspended parallel mechanism while considering cable mass," *Mechanism and Machine Theory*, vol. 66, pp. 1–13, 2013.
7. H.Yuan, E. Courteille, and D. Deblaise, "Static and dynamic stiffness analyses of cable-driven parallel robots with non-negligible cable mass and elasticity," *Mechanism and Machine Theory*, vol. 85, pp. 64–81, 2015.
8. H.Yuan, E. Courteille, M. Gouttefarde, and P.-E. Hervé, "Vibration analysis of cable-driven parallel robots based on the dynamic stiffness matrix method," *Journal of Sound and Vibration*, vol. 394, pp. 527–544, 2017.
9. M. Anson, A. Alamdari, and V. Krovi, "Orientation workspace and stiffness optimization of cable-driven parallel manipulators with base mobility," *ASME Journal of Mechanisms and Robotics*, vol. 9, 2017.
10. S. Abdolshah, D. Zanotto, G. Rosati, and S. K. Agrawal, "Optimizing stiffness and dexterity of planar adaptive cable-driven parallel robots," *ASME Journal of Mechanisms and Robotics*, vol. 9, 2017.
11. H. Jamshidifar, A. Khajepour, B. Fidan, and M. Rushton, "Kinematically-constrained redundant cable-driven parallel robots: Modeling, redundancy analysis, and stiffness optimization," *IEEE/ASME Transactions on Mechatronics*, vol. 22, no. 2, pp. 921–930, April 2017.
12. C. Nelson, "On improving stiffness of cable robots," in *Cable-Driven Parallel Robots - Proceedings of the 3rd International Conference on Cable-Driven Parallel Robots*, ser. Mechanisms and Machine Science, vol. 53. Netherlands: Springer Netherlands, 2018, pp. 331–339.
13. M. Gouttefarde and C. M. Gosselin, "Analysis of the wrench-closure workspace of planar parallel cable-driven mechanisms," *IEEE Transactions on Robotics*, vol. 22, no. 3, pp. 434–445, June 2006.
14. P. Bosscher, A. T. Riechel, and I. Ebert-Uphoff, "Wrench-feasible workspace generation for cable-driven robots," *IEEE Transactions on Robotics*, vol. 22, no. 5, pp. 890–902, Oct 2006.